PLOS ONE

RESEARCH ARTICLE

Growth, ammonium metabolism, and photosynthetic properties of *Ulva australis* (Chlorophyta) under decreasing pH and ammonium enrichment

Leah B. Reidenbach[1¤a]*, Pamela A. Fernandez[2¤b], Pablo P. Leal[2¤c], Fanny Noisette[2,3], Christina M. McGraw[2,4], Andrew T. Revill[5], Catriona L. Hurd[2], Janet E. Kübler[1]

1 Department of Biology, California State University at Northridge, Northridge, California, United States of America, **2** Institute for Marine and Antarctic Studies, University of Tasmania, Hobart, Tasmania, Australia, **3** GEOMAR Helmholtz Centre for Ocean Research, Kiel, Germany, **4** Department of Chemistry, University of Otago, Dunedin, New Zealand, **5** CSIRO, Oceans and Atmosphere, Hobart, Tasmania, Australia

¤a Current address: School of Marine and Atmospheric Sciences, Stony Brook University, Stony Brook, New York, United States of America
¤b Current address: Centro i~mar, Universidad de Los Lagos, Puerto Montt, Chile
¤c Current address: Instituto de Fomento Pesquero, Puerto Montt, Chile
* Leah.Reidenbach@stonybrook.edu

Citation: Reidenbach LB, Fernandez PA, Leal PP, Noisette F, McGraw CM, Revill AT, et al. (2017) Growth, ammonium metabolism, and photosynthetic properties of *Ulva australis* (Chlorophyta) under decreasing pH and ammonium enrichment. PLoS ONE 12(11): e0188389. https://doi.org/10.1371/journal.pone.0188389

Editor: Bayden D. Russell, The University of Hong Kong, HONG KONG

Received: April 6, 2017

Accepted: November 6, 2017

Published: November 27, 2017

Data Availability Statement: All data files are available from the CSUN ScholarWorks Open Access Repository (SOAR) (http://hdl.handle.net/10211.3/195049).

Funding: This work was supported by National Science Foundation grant: OISE 1515267 (URL: https://www.nsf.gov/awardsearch/showAward?AWD_ID=1515267) (Author: LBR). The funders had no role in study design, data collection and

Abstract

The responses of macroalgae to ocean acidification could be altered by availability of macronutrients, such as ammonium (NH_4^+). This study determined how the opportunistic macroalga, *Ulva australis* responded to simultaneous changes in decreasing pH and NH_4^+ enrichment. This was investigated in a week-long growth experiment across a range of predicted future pHs with ambient and enriched NH_4^+ treatments followed by measurements of relative growth rates (RGR), NH_4^+ uptake rates and pools, total chlorophyll, and tissue carbon and nitrogen content. Rapid light curves (RLCs) were used to measure the maximum relative electron transport rate ($rETR_{max}$) and maximum quantum yield of photosystem II (PSII) photochemistry (F_v/F_m). Photosynthetic capacity was derived from the RLCs and included the efficiency of light harvesting (α), slope of photoinhibition (β), and the light saturation point (E_k). The results showed that NH_4^+ enrichment did not modify the effects of pH on RGRs, NH_4^+ uptake rates and pools, total chlorophyll, $rETR_{max}$, α, β, F_v/F_m, tissue C and N, and the C:N ratio. However, E_k was differentially affected by pH under different NH_4^+ treatments. E_k increased with decreasing pH in the ambient NH_4^+ treatment, but not in the enriched NH_4^+ treatment. NH_4^+ enrichment increased RGRs, NH_4^+ pools, total chlorophyll, $rETR_{max}$, α, β, F_v/F_m, and tissue N, and decreased NH_4^+ uptake rates and the C:N ratio. Decreased pH increased total chlorophyll content, $rETR_{max}$, F_v/F_m, and tissue N content, and decreased the C:N ratio. Therefore, the results indicate that *U. australis* growth is increased with NH_4^+ enrichment and not with decreasing pH. While decreasing pH influenced the carbon and nitrogen metabolisms of *U. australis*, it did not result in changes in growth.

analysis, decision to publish, or preparation of the manuscript.

Competing interests: The authors have declared that no competing interests exist.

Introduction

Since the industrial revolution, the atmospheric CO_2 concentration has increased from 280 μatm to over 390 μatm, and about 30% of the additional CO_2 has been absorbed by the ocean [1]. This results in ocean acidification, a term which describes the contemporary reduction in seawater pH by ca. 0.1 units with an expected further reduction of 0.3–0.5 units by 2100 [2–5]. In addition to ocean acidification, coastal regions receive inputs of excess nitrogen from aquaculture, agriculture, wastewater treatment, and the burning of fossil fuels [6,7]. Excess nitrogen is the commonly regarded cause for green algal blooms world-wide, and they are typically dominated by macroalgae from the genus *Ulva* [8–10]. Green algal blooms can impose negative effects on their ecosystems and local human communities by decreasing biodiversity and ecosystem services [11–14]. Elevated nutrients can modify the effects of elevated pCO_2/decreased pH on algal physiology [15–22] because nitrogen and carbon metabolisms are linked via the process of protein synthesis [23]. In order to understand how nutrient-opportunistic macroalgae, such as *Ulva* spp. will respond to future oceanic conditions, it is important to consider the interaction of elevated nutrients with decreasing pH.

Non-calcareous macroalgae have been shown to express a range of responses to future pCO_2/pH conditions. *Hizikia fusiforme* growth rates increased under future pCO_2/pH conditions while maximum photosynthetic rates were unchanged [24]. Growth rates of *Gracilaria chilensis* and another *Gracilaria* sp. were enhanced by future pCO_2/pH conditions [25]. *Gracilaria lemaneiformis* growth rates were also enhanced under future pCO_2/pH conditions, but only at an intermediate photon flux density (PFD) (160 μM photons m^{-2} s^{-1}) [26]. The growth rates of thirteen species of algae, including green, red, and brown algae, had no response to future pCO_2/pH conditions with the exception of *Hypnea musciformis*, which exhibited negative growth rates [27]. *Ulva* spp. growth rates have been shown to increase or be unaffected by future pCO_2/pH conditions [21,28–30]. Differences in responses to elevated pCO_2/decreased pH may be caused in part by species specific differences or by unsuitable nutrient concentrations, temperature, and/or PFD for the seaweeds to support higher growth rates.

Carbon concentrating mechanisms (CCMs) allow macroalgae to increase CO_2 at the site of carbon fixation and may be downregulated with elevated pCO_2/decreased pH in *Ulva* spp. [31,32]. This has been linked to increased energy availability for nutrient uptake, protein synthesis, and growth when nutrients are not limiting [31,33,34]. Therefore, elevated pCO_2/decreased pH might change nutrient uptake, assimilation, and storage capacity of macroalgae which utilize CCMs. For example, when CCMs were reduced with elevated pCO_2/decreased pH in *Pyropia haitanensis*, growth rates and NO_3^- uptake rates increased, and photosynthetic rates increased with the combination of elevated pCO_2 and elevated NO_3^- [35]. Further, nutrients mediated the effect of elevated pCO_2/decreased pH on *P. haitanensis* by increasing growth rates and nitrate reductase activity (NRA) when grown with elevated CO_2 and NO_3^- enrichment [20]. *Ulva lactuca* photosynthetic rates and NRA were increased with elevated pCO_2/decreased pH, but only when temperature was sufficient (25˚C compared to 15˚C), while NO_3^- uptake rates were enhanced at both temperatures with elevated pCO_2/decreased pH [21]. Another algal species which utilizes CCMs, *Hizikia fusiforme*, was also found to have enhanced growth rates, NRA, and nitrate uptake rates with elevated pCO_2/decreased pH [24]. The interaction of NH_4^+ enrichment and elevated pCO_2/decreased pH increased growth rates of *Ulva pertusa* [22]. These studies provide evidence that local (i.e., nutrient enrichment) and global (i.e., ocean acidification) drivers of environmental change could interact to change macroalgal growth and physiology.

Ulva spp. are opportunistic under eutrophic conditions [9] and have potentially increased growth rates under elevated pCO_2 alone [15,28]. Prior studies suggest nitrogen in the form of

NO_3^- could have interacting effects with elevated pCO_2/decreased pH in *Ulva* spp., but less is known regarding the effects of NH_4^+ as a potential interacting driver [15,16,22,32]. Typically, NH_4^+ is the preferred form of nitrogen for *Ulva* spp. because it requires less energy for assimilation than NO_3^-, as NO_3^- must first be reduced via nitrate reductase activity (NRA) [36]. Although NO_3^- is the most abundant and common form of dissolved inorganic nitrogen (DIN) in the ocean, increasing human population densities on coasts, land use change, and decreasing ocean pH all increase the availability of NH_4^+ in coastal areas [37].

To test the hypothesis that there will be an interacting effect of decreasing pH and elevated NH_4^+ concentrations on the growth, nutrient, and photosynthetic physiology of *Ulva australis*, a laboratory growth experiment was conducted across a range of future pCO_2/pH conditions (total scale pH (pH_T): 7.56–7.85) under ambient and elevated NH_4^+ concentrations. This was followed by measurements of RGRs, NH_4^+ uptake rates and pools, total chlorophyll, tissue carbon and nitrogen content, and photosynthetic characteristics of photosystem II using PAM fluorometry. Multiple components of carbon and nitrogen metabolisms were measured with the aim of describing how changes in these processes integrate at the organismal level (i.e., growth). With elevated pCO_2/decreased pH and NH_4^+ enrichment *Ulva* spp. should have adequate internal supply of nitrogenous and carbon skeleton precursors and may have increased growth rates, potentially leading to increases in the severity of frequency of green tide blooms.

Methods

Collection and acclimation

Ulva australis was collected from Blackmans Bay, Tasmania, Australia (42˚59'56"S 147˚19'8"E) in July 2015 (Austral winter). Algae were stored in plastic zip-lock bags with seawater on ice and transported to the laboratory in a cooler within five hours of collection. *U. australis* was identified using morphological characteristics. All visible epiphytes were carefully removed from the surface of the blades which were then rinsed with filtered seawater. The cleaned algal samples were kept in aerated seawater at 16.6˚C under 200 μmol photons m^{-2} s^{-1} (measured using a 4π Li-Cor LI-193 Spherical Quantum Sensor connected to a LI-250A portable light meter) with a 12h:12h light dark cycle for 3 days to acclimate to experimental light and temperature conditions.

Experimental design

Three *Ulva australis* thalli with a total fresh weight of 1.07 ± 0.02 g (mean ± SEM) were placed in 650 mL chambers filled with 600 mL of seawater that was UV-sterilized and filtered through a 1 μm-filter (Polyester Felt Filter Bags, NETCO, Hobart, Australia). Peristaltic pumps (FPU500, Omega Engineering, USA) were used to provide fresh seawater to each of the 24 growth chambers at a rate of 6–8 mL/min. The pH_T of seawater pumped to each tank was maintained using an automated pH control system [38]. Seawater was equilibrated using a membrane contactor (Micromodule, model 0.5X1, Membrana, USA) where the appropriate mix of N_2 and CO_2 gas was achieved using three pairs of mass flow controllers (MFCs) set to pH_Ts of 8.05, 7.85, and 7.65 (FMA5418A and FMA545C, Omega Engineering, USA). The flow rate of each MFC was proportional to the input voltage, which was supplied by an analog output module housed in a USB chassis (NI9264 and cDAQ-9174, National Instruments, USA) using a control system similar to that described in Bockman [39].

Each of the three MFCs were randomly assigned to four ambient NH_4^+ and four enriched NH_4^+ growth chambers for a total of 24 chambers. The pH_T within each culture chamber was measured every 1.5–3 hours throughout the week-long experiment, monitoring the effect of *U. australis* photosynthesis and respiration on seawater pH_T. The seaweed biomass: seawater

volume ratio affected the pH_T of the culture chambers so the average pH_T of each chamber was denoted by measurements of pH_T during the dark cycle throughout the entire experiment which resulted in a continuous range of pH_Ts (7.56–7.85) representative of future seawater pH conditions.

The ambient NH_4^+ concentration (n = 12) served as a control for the nutrient treatment and consisted of natural, UV-sterilized, filtered seawater. The elevated concentration of NH_4^+ (n = 12) was achieved using an auto-dosing peristaltic pump (Jebao DP-4) programmed to deliver 12 mL of a 1000 μM NH_4Cl solution to growth chambers every two hours. Based on NH_4^+ dosing rate, the NH_4^+ concentration in the elevated treatment was 20 μM. However, discrete measurements of seawater NH_4^+ concentrations on days 0, 3, and 6 showed that the average NH_4^+ concentration was 0.4 ± 0.3 μM in the ambient treatment and 38.0 ± 18.6 μM the enriched treatment.

pH_T and total alkalinity measurements

A syringe pump (V6 pump with valve 24090, Norgren, UK) and two 12-port rotary valves (23425 valve driver with valve 24493, Norgren, UK) were used to sample seawater directly from each growth chamber. For each spectrophotometric pH measurement, a reference spectrum was acquired after flushing 25 mL of seawater through a 1 cm flow-through quartz cuvette. A spectrum (400–800 nm) was acquired using an LED light source and a UV-Vis spectrometer (BluLoop and USB2000+, Ocean Optics, USA). A dye + seawater spectrum was then obtained after mixing 200 μL of 2 mM metacresol purple sodium salt dye (211761-10G, Sigma Aldrich, Australia) with an additional 25 mL of seawater within the syringe pump. The two spectra were used to calculate an absorbance spectrum. pH_T was calculated using the quadratic fits of the absorbance spectra between 429–439 nm, 573–583 nm and a background signal averaged between 750–760 nm. When compared to calculations based on a single wavelength, the quadratic fit approach leads to a three-fold improvement in measurement precision [38]. Each recorded pH_T was the average of four replicate measurements, which took approximately three minutes to obtain. The temperature of each sample was recorded with a PT100 temperature sensor and a high-precision data logger (PT-104, PICO Technology, UK). All instrument control, spectra manipulations, and pH_T calculations were done using LabVIEW 2014 (National Instruments, USA).

Total alkalinity (AT) samples were calculated from water samples collected in October 2015 using seawater from the same region (Taroona, Tasmania, Australia) as was collected in July 2015 for the experiment. AT samples were poisoned with mercuric chloride (0.02% vol/vol [40]) and were analyzed at the Australian National University, using an automatic built in-house titrator (consisting of a 5 mL Tecan syringe pump (Cavro X Calibur Pump), a Pico USB controlled pH sensor, and a TPS pH electrode). AT values were then calculated using the Gran technique [40].

Growth rates

Ulva australis thalli were blotted with tissue to remove excess water and weighed before the start of the experiment and after seven days. The total weight of the three thalli from each chamber was used for the analysis. The RGR, expressed as % day^{-1}, was calculated as $RGR = \ln(FW_f/FW_i) \times t^{-1} \times 100$ where FW_i is the initial fresh weight, and FW_f is the final fresh weight after t days.

NH_4^+ uptake rates

At the end of the seven-day incubation period, one of the three *Ulva australis* thalli (0.43 ± 0.03 g of FW) was removed from each chamber to an Erlenmeyer flask containing 200 mL of

filtered seawater with overhead light of 200 μmol photons m^{-2} s^{-1}. The seawater in each flask was obtained from the automated pH control system shortly before the start of the experiment so the seawater pH_T in the flasks was representative of the seawater in the chambers the algae came from. The initial NH_4^+ concentration of 20 μM was obtained with the addition of NH_4Cl to ambient seawater. Flasks were placed on an orbital shaker (RATEK OM7, Victoria, Australia) set to 80 rpm and continuously stirred to induce water motion and reduce boundary layer effects [41]. A 10 mL sample of the water was taken at 0 and 30 minutes, and frozen at -20˚C, until defrosted and analyzed for NH_4^+ concentration using a QuickChem 8500 series 2 Automated Ion Analyzer (Lachat Instrument, Loveland, USA). The uptake rate (V) was determined according to Pedersen [42]] using the formula $V = [(S_i \times vol_i)\text{-}(S_f \times vol_f)]/(t \times FW)$ where S_i and S_f are the initial and final NH_4^+ concentrations (μM) over a period of time (t), vol is the seawater volume in the flask and FW is the fresh weight (g) of the algae.

Internal soluble NH_4^+ pools

The boiling water extraction method was used to determine the internal soluble NH_4^+ pool [43]. *Ulva australis* tissue (0.18 ± 0.01 g FW) was put in a boiling tube with 20 mL of deionized water then placed in a boiling water bath for 40 minutes. The liquid was cooled, decanted, and then filtered through a 0.45 μm Whatman filter (GF/C). This process was repeated on the same algal piece three times and the concentration of internal soluble NH_4^+ pools was calculated using the sum of the NH_4^+ concentrations of the three water samples of each algal piece. NH_4^+ concentrations were measured as stated above.

Photosynthetic pigments

Following the experiment, a 0.04 ± 0.001 g FW piece of *Ulva australis* from each experimental chamber was kept at -20˚C pending analysis. Each sample was then ground in 5 mL of 100% ethanol with a ceramic mortar and pestle in dim light and with the samples shaded. The extract was poured into 10 mL centrifuge tubes and placed in the dark at 4˚C for six hours. Samples were then centrifuged for 10 min at 4000 rpm at 4˚C. Total Chl *a* and *b* concentrations in the supernatant were determined according to the quadrichroic formula from Ritchie [44] using a spectrophotometer (S-22 UV/Vis, Boeco, Germany).

Rapid light curves

Chlorophyll fluorescence of photosystem II was measured using a Pulse Amplitude Modulation fluorometer (diving-PAM, Walz, Germany) to generate rapid light curves and obtain measurements of the maximum quantum yield of PSII photochemistry (F_v/F_m), which is used as an indicator of stress [45]. On day seven of the experiment, one thallus from each chamber was dark adapted for 20 minutes before exposure to a flash of saturating light to obtain maximum fluorescence (F_m). Then a rapid light curve was generated by increasing exposure to photosynthetic active radiation (PAR) ranging from 0–422 μM photons m^{-2} s^{-1}. F_v/F_m was calculated by the equation $F_m\text{-}F_0/F_m$, were F_0 is the fluorescence under measuring light conditions (ca. 0.15 μmol photons m^{-2} s^{-1}) and F_m is the maximum fluorescence under saturating light conditions. Relative ETR (rETR) was calculated by the equation rETR = Y * PAR * 0.5. A hyperbolic curve was fit to the rETRs generated by each rapid light curve using a modified equation of Walsby [46]:

$$rETR_c = rETR_{max}\left(1 - \exp\left(-\frac{\alpha I}{P_m}\right)\right) + \beta I$$

where $rETR_c$ is the calculated rETR, $rETR_{max}$ is the maximum ETR at light saturating PFDs, α is the initial slope of the curve during light-limiting PFDs, and β is the slope of photoinhibition at high PFDs. The coefficients used in the equation were calculated using a least squares method [46].

Total carbon and nitrogen content

A 0.35 ± 0.03 g FW section was dried at 60˚C overnight, ground to a fine powder, and then analyzed for total tissue carbon and nitrogen content. Samples were weighed into pressed tin capsules (5x8 mm, 0.2 mg; Sercon, U.K.). Carbon and nitrogen content were determined using a Fisons NA1500 elemental analyzer coupled to a Thermo Scientific Delta V Plus via a Conflo IV. Combustion and reduction were achieved at 1020˚C and 650˚C respectively. Percent C and N composition was calculated by comparison of mass spectrometer peak areas to those of standards with known concentrations.

Data analysis

An analysis of covariance (ANCOVA) was used to test for the interacting effect of pH and NH_4^+ on physiological responses of *U. australis*. pH_T was used as the continuous factor (i.e., the covariate) and NH_4^+ was used as the categorical variable. The relationships of each physiological response with decreasing pH in both ambient and enriched NH_4^+ treatments were compared to determine if the NH_4^+ treatment (ambient or enriched) altered the effect of decreased pH_T. First, the interacting term was tested to determine if the slopes of the NH_4^+ treatments were equal. The interaction term was dropped from the ANCOVA model if the slopes were equal (i.e., $p > 0.05$ for the interaction term) to test for the effects of increased pCO_2/decreased pH and NH_4^+ enrichment. Outliers greater than 3 standard deviations from the mean were removed *a priori* and are indicated in the figures. ANCOVA assumptions were checked using a Shapiro-Wilk test of normality and Cochran's Q test for homogeneity of variances. Tissue N and NH_4^+ pools were log transformed to meet assumption of normality. Statistical analyses were done using the statistical software R studio.

Results

Total pH and seawater carbonate parameters

The pH_T given for each treatment is the average value from the dark cycle pH_T measurements in each culture chamber. The measurements oscillated around the gas mixers' set points due to algal metabolism: during the light period pCO_2 decreased, increasing pH_T; during the dark period cellular respiration produced CO_2, decreasing pH_T, with pH_T being relatively stable throughout the dark cycle (Fig 1). Dark cycle pH_T values were correlated to light and whole cycle pH_T values (Pearson correlation: $r = 0.70$, $p = 0.0002$ and $r = 0.92$, $p < 0.0001$, respectively). Mean values for each chamber during light, dark, and whole day cycles throughout the experiment are reported in Table 1. Seawater carbonate parameters are described in the S1 Table.

Interactive effects

The slopes for all dependent variables, with the exception of E_k, were indistinguishable between ambient and enriched NH_4^+ treatments as indicated by the non-significant interaction terms (pH_T and NH_4^+) in the ANCOVAs (Table 2). The following results of those dependent variables with a non-significant interaction are reported as ANCOVAs with the interacting term dropped from the model.

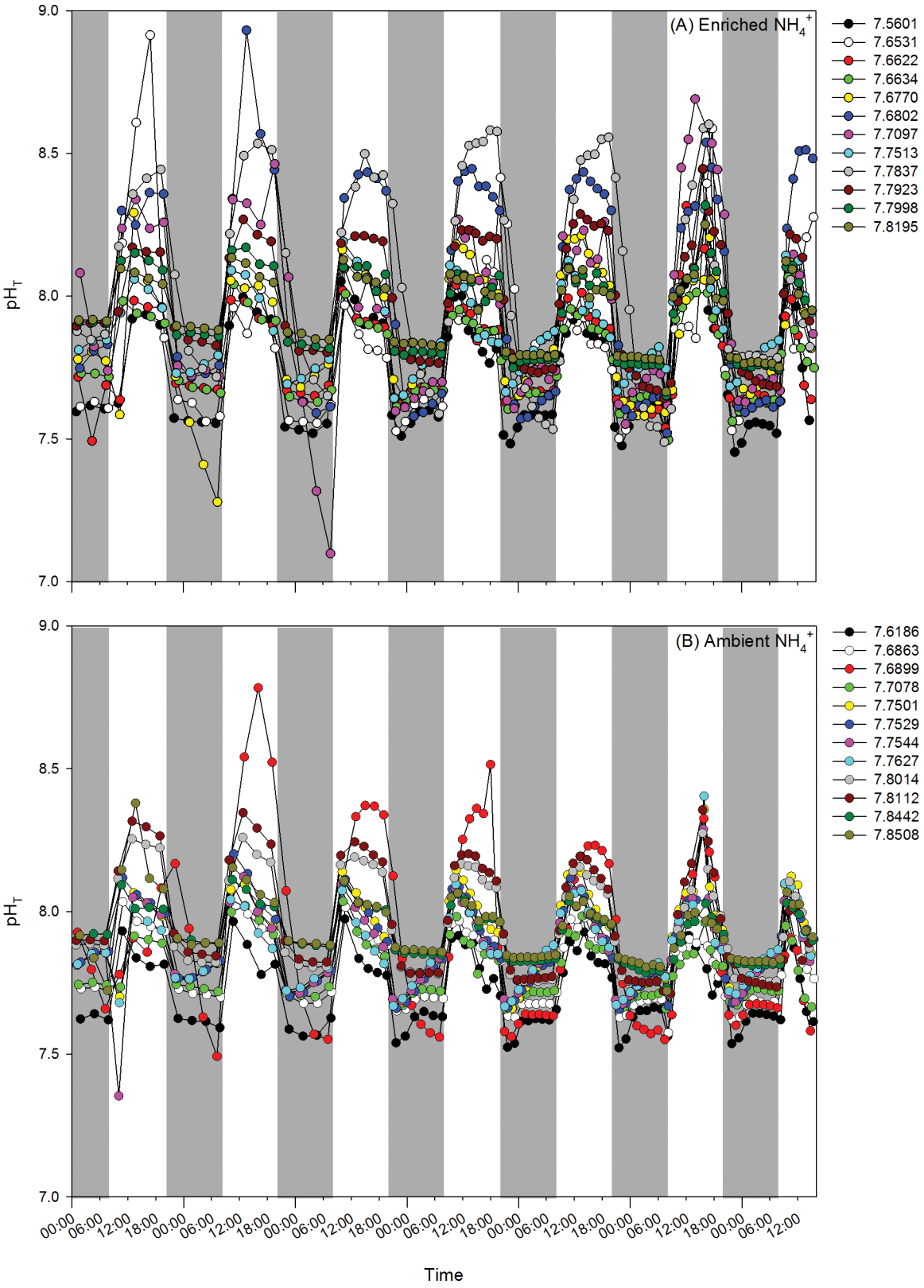

Fig 1. Seven day pH_T regime for each chamber for (A) enriched NH_4^+ treatments (n = 12) and (B) ambient NH_4^+ treatments (n = 12). The pH monitoring system took pH_T measurements of each *U. australis* growth chambers every 1.5–3 hours. Shaded areas of the graph represent dark periods.

https://doi.org/10.1371/journal.pone.0188389.g001

Table 1. Mean and confidence intervals (CI: Mean [H+] ± (-log (SEM of [H+]))) for pH_T of each chamber for light, dark, and whole day cycles. n = number of samples collected during cycle throughout experiment.

MFC	NH_4^+	Light Cycle pH_T	n	Dark Cycle pH_T*	n	Whole Day pH_T	n
1	Ambient	7.92 (7.88, 7.96)	50	7.69 (7.67, 7.71)	39	7.81 (7.79, 7.84)	92
1	Ambient	7.82 (7.81, 7.84)	50	7.71 (7.70, 7.71)	36	7.78 (7.77, 7.79)	92
1	Ambient	7.77 (7.75, 7.78)	50	7.62 (7.61, 7.63)	39	7.70 (7.69, 7.71)	92
1	Ambient	7.85 (7.83, 7.86)	50	7.69 (7.68, 7.69)	38	7.78 (7.76, 7.79)	92
1	Enriched	7.83 (7.80, 7.85)	50	7.56 (7.55, 7.57)	39	7.69 (7.68, 7.71)	92
1	Enriched	7.84 (7.81, 7.86)	50	7.66 (7.65, 7.67)	38	7.76 (7.74 7.78)	91
1	Enriched	7.85 (7.82, 7.88)	50	7.65 (7.63, 7.67)	38	7.76 (7.74, 7.78)	92
1	Enriched	7.85 (7.83, 7.86)	50	7.66 (7.65, 7.67)	40	7.76 (7.74, 7.77)	92
2	Ambient	7.92 (7.89, 7.95)	48	7.75 (7.75, 7.76)	37	7.84 (7.83, 7.86)	90
2	Ambient	7.93 (7.91, 7.95)	49	7.76 (7.75, 7.77)	37	7.85 (7.84, 7.86)	91
2	Ambient	7.95 (7.93, 7.98)	49	7.75 (7.74, 7.76)	35	7.86 (7.85, 7.88)	91
2	Ambient	7.95 (7.94, 7.97)	46	7.75 (7.74, 7.76)	38	7.86 (7.84, 7.87)	87
2	Enriched	7.92 (7.87, 7.96)	49	7.68 (7.66, 7.69)	35	7.81 (7.78, 7.83)	91
2	Enriched	7.93 (7.90, 7.97)	50	7.75 (7.74, 7.76)	36	7.85 (7.83,7.87)	91
2	Enriched	8.09 (8.04, 8.15	49	7.68 (7.66, 7.70)	37	7.88 (7.85,7.91)	91
2	Enriched	7.97 (7.91, 8.04)	50	7.71 (7.68, 7.74)	38	7.85 (7.81, 7.88)	91
3	Ambient	8.04 (8.01, 8.06)	50	7.80 (7.79, 7.81)	39	7.92 (7.91, 7.94)	92
3	Ambient	8.05 (8.03. 8.08)	50	7.81 (7.80, 7.82)	39	7.93 (7.92, 7.95)	92
3	Ambient	7.97 (7.95, 7.98)	51	7.84 (7.84, 7.85)	36	7.92 (7.91, 7.92)	91
3	Ambient	7.97 (7.96, 7.99)	50	7.85 (7.85, 7.86)	36	7.92 (7.91, 7.93)	92
3	Enriched	8.06 (8.03, 8.09)	50	7.79 (7.78, 7.81)	38	7.93 (7.91, 7.95)	92
3	Enriched	8.07 (8.02, 8.12)	50	7.78 (7.75, 7.81)	37	7.94 (7.91, 7.97)	92
3	Enriched	7.99 (7.98, 8.01)	51	7.82 (7.81, 7.83)	36	7.92 (7.90, 7.93)	91
3	Enriched	8.00 (7.98, 8.02)	51	7.80 (7.79, 7.81)	36	7.91 (7.90, 7.93)	91

* The dark cycle pH_T averages were calculated throughout the last 11 hours of the dark cycle.

https://doi.org/10.1371/journal.pone.0188389.t001

Growth rates

RGRs of *Ulva australis* in enriched NH_4^+ treatments (8.75 ± 0.69% day^{-1}, mean ± SEM) were approximately double those in the ambient NH_4^+ treatments (4.36 ± 0.5% day^{-1}) (ANCOVA; $F_{1, 21} = 25.60$, $p < 0.001$, Fig 2). RGRs did not differ across pH_T treatments (ANCOVA; $F_{1, 21} = 2.09$, $p = 0.1630$).

NH_4^+ uptake rates

NH_4^+ uptake rates were higher in *Ulva australis* from the enriched NH_4^+ treatment (9.06±1.04 μmol NH_4^+ g^{-1} FW $hour^{-1}$) than in the ambient NH_4^+ treatment (13.42±0.97 μmol NH_4^+ g^{-1} FW $hour^{-1}$) (ANCOVA; $F_{1, 21} = 8.9374$, $p = 0.007$, Fig 3A). pH_T had no significant effect on the NH_4^+ uptake rates (ANCOVA; $F_{1, 21} = 0.9148$, $p = 0.3497$).

Internal NH_4^+ pools

Internal NH_4^+ pools in *Ulva australis* thalli were higher in the enriched NH_4^+ treatments (75.21 ± 8.85 μmol NH_4^+ g^{-1} FW) than in the ambient NH_4^+ treatment (39.60 ± 4.81 μmol NH_4^+ g^{-1} FW) (ANCOVA; $F_{1, 20} = 13.6771$, $p = 0.0041$, Fig 3B). pH_T had no effect on the NH_4^+ pools (ANCOVA; $F_{1, 20} = 0.0007$, $p = 0.9789$).

Table 2. ANCOVA results for *Ulva australis*.

		Full Model[a]				Partial Model[b]			
Variable	Source of Variation	Degrees of Freedom	F-value	p-value*	Model R^2 (p-value)*	Degrees of Freedom	F-value	p-value*	Model R^2 (p-value)*
RGR	pH	1	2.0011	0.1726	0.571	1	2.0900	0.1630	0.5687
	NH_4^+	1	24.5112	0.0001	(**<0.0001**)	1	25.6000	**0.0001**	(**<0.0001**)
	pH x NH_4^+	1	0.1070	0.7470					
	Residuals	20				21			
NH_4^+	pH	1	0.8715	0.3617	0.3195	1	0.9148	0.3497	0.3193
uptake	NH_4^+	1	8.5138	0.0085	(**0.0485**)	1	8.9374	**0.0070**	(**0.01761**)
rates	pH x NH_4^+	1	0.0048	0.9455					
	Residuals	20				21			
NH_4^+	pH	1	0.0007	0.9794	0.4094	1	0.0007	0.9789	0.4061
pools	NH_4^+	1	13.0640	0.0018	(**0.0165**)	1	13.6771	**0.0014**	(**0.0055**)
	pH x NH_4^+	1	0.1035	0.7511					
	Residuals	19				20			
Total	pH	1	6.7120	0.0175	0.4865	1	7.0470	**0.0148**	0.4864
Chl	NH_4^+	1	12.2325	0.0023	(**0.0034**)	1	12.8430	**0.0018**	(**0.0009**)
	pH x NH_4^+	1	0.0018	0.9669					
	Residuals	20				21			
$rETR_{max}$	pH	1	11.9689	0.0025	0.7062	1	12.4760	**0.0020**	0.704
	NH_4^+	1	35.9519	<0.0001	(**<0.0001**)	1	37.4740	**<0.0001**	(**<0.0001**)
	pH x NH_4^+	1	0.1473	0.7052					
	Residuals	20				21			
E_k	pH	1	4.4425	0.0479	0.3164	—	—	—	—
	NH_4^+	1	0.8463	0.0385	(0.0506)	—	—	—	
	pH x NH_4^+	1	4.7757	**0.0409**					
	Residuals	20				—			
α	pH	1	0.0001	0.9936	0.3342	1	0.0001	0.9938	0.2565
	NH_4^+	1	7.7059	0.0117	(**0.0397**)	1	7.2452	**0.0137**	(**0.0445**)
	pH x NH_4^+	1	2.3354	0.1421					
	Residuals	20				21			
β	pH	1	0.0215	0.8850	0.4442	1	0.0195	0.8902	0.3581
	NH_4^+	1	12.8634	0.0018	(**0.0073**)	1	11.6938	**0.0026**	(**0.0095**)
	pH x NH_4^+	1	3.1003	0.0936					
	Residuals	20				21			
F_v/F_m	pH	1	10.4249	0.0042	0.6712	1	10.5410	**0.0039**	0.6586
	NH_4^+	1	29.6389	<0.0001	(**<0.0001**)	1	29.9680	**<0.0001**	(**<0.0001**)
	pH x NH_4^+	1	0.7693	0.3909					
	Residuals	20				21			
%N	pH	1	5.7027	0.0269	0.7761	1	5.6892	**0.0266**	0.7643
	NH_4^+	1	62.5572	<0.0001	(**<0.0001**)	1	62.4082	**<0.0001**	(**<0.0001**)
	pH x NH_4^+	1	1.0501	0.3177					
	Residuals	20				21			
%C	pH	1	0.5404	0.4708	0.1021	1	0.5377	0.4715	0.05263
	NH_4^+	1	0.6318	0.4360	(0.5307)	1	0.6288	0.4367	(0.5669)
	pH x NH_4^+	1	1.1022	0.3063					
	Residuals	20				21			
C:N	pH	1	6.8442	0.0165	0.793	1	6.9056	**0.0157**	0.7846

(*Continued*)

Table 2. (*Continued*)

		Full Model[a]				Partial Model[b]			
Variable	**Source of Variation**	**Degrees of Freedom**	**F-value**	**p-value***	**Model R^2 (p-value)***	**Degrees of Freedom**	**F-value**	**p-value***	**Model R^2 (p-value)***
	NH_4^+	1	68.9589	0.0000	(**<0.0001**)	1	69.5776	**0.0000**	(**<0.0001**)
	pH x NH_4^+	1	0.8133	0.3779					
	Residuals	20				21			

RGR, relative growth rate; Chl, Chlorophyll; $rETR_{max}$, maximum relative electron transport rate; E_K, light saturation point; α, the efficiency of light harvesting; β, slope of photoinhibition; F_v/F_m, maximum quantum yield of PSII photochemistry; %N, percent tissue nitrogen; % C, percent tissue carbon; C:N, carbon to nitrogen ratio.

*p-values in bold indicate significance (α = 0.05).

[a]The full model ANCOVA included the interaction term (pH x NH_4^+) to test for differences in the slopes.

[b]If the interaction was non-significant, the partial model ANCOVA including only NH_4^+ (the categorical variable) and the covariate pH (the continuous variable) as factors was used.

https://doi.org/10.1371/journal.pone.0188389.t002

Photosynthetic pigments

The total chlorophyll concentration (Chl *a* + *b*) content was higher in *Ulva australis* from enriched NH_4^+ treatments (1.27±0.07 mg g^{-1} FW) compared to the ambient NH_4^+ treatment (0.86±0.08 mg g^{-1} FW) (ANCOVA; $F_{1, 21} = 12.8430$, p = 0.0018, Fig 4A). The total chlorophyll concentration also increased with decreasing pH_T (ANCOVA; $F_{1, 21} = 7.0470$, p = 0.0148).

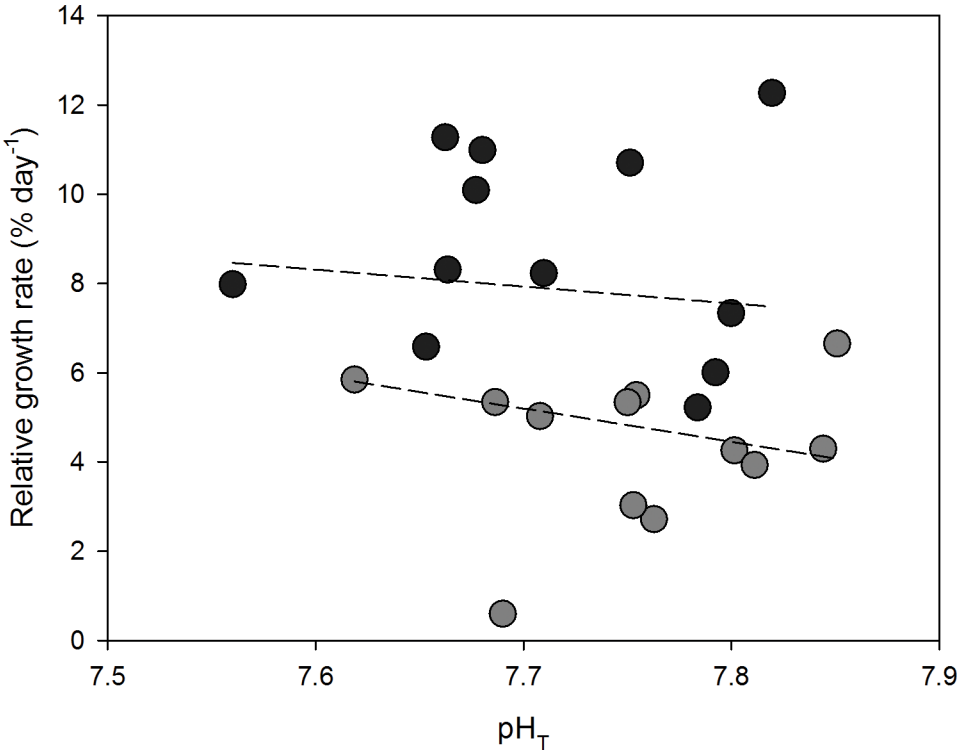

Fig 2. Relative growth rates (% day^{-1}) for *Ulva australis* under ambient and enriched NH_4^+ treatments across a range of pH_T. Grey points represent ambient NH_4^+ treatments and black points represent enriched NH_4^+ treatments. The slope of RGR with decreasing pH_T for each NH_4^+ treatment (dashed lines) were tested for an interaction using an ANCOVA.

https://doi.org/10.1371/journal.pone.0188389.g002

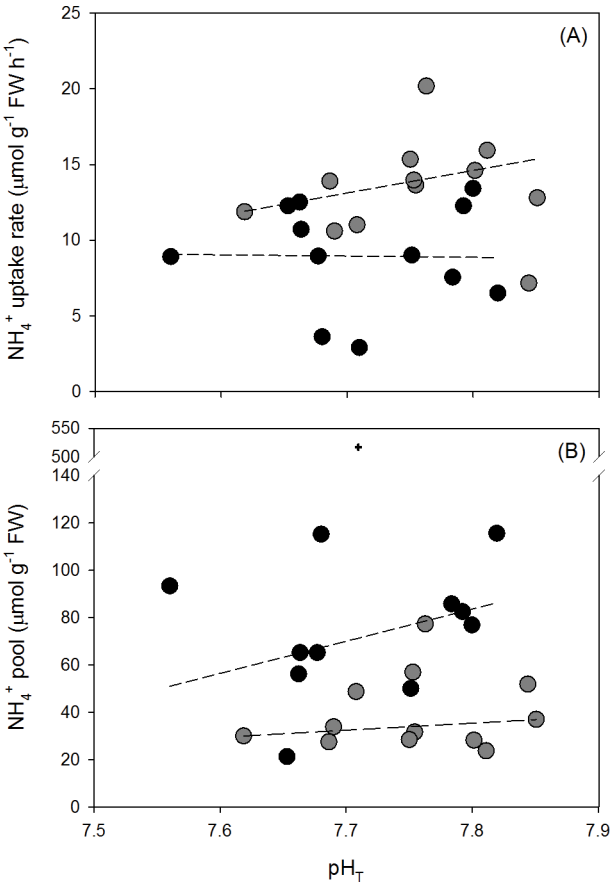

Fig 3. (A) NH_4^+ uptake rates (µmol g^{-1} FW $hour^{-1}$) in 20 µM NH_4^+ seawater for 30 minutes and (B) internal NH_4^+ pools (µmol g^{-1} FW) for *Ulva australis* grown under ambient and enriched NH_4^+ treatments across a range of pH_Ts. Grey points represent ambient NH_4^+ treatments and black points represent enriched NH_4^+ treatments. A plus symbol (+) indicates an outlier which was removed for statistical analysis. The slopes of NH_4^+ uptake rates and internal NH_4^+ pools with pH_T for each NH_4^+ treatment (dashed lines) were tested for an interaction using an ANCOVA.

https://doi.org/10.1371/journal.pone.0188389.g003

Rapid light curves

$rETR_{max}$ increased with NH_4^+ enrichment (ANCOVA; $F_{1, 21} = 37.4740$, $p<0.001$, Fig 4B) with an average $rETR_{max}$ of 4.96±0.58 in the ambient NH_4^+ treatment and 11.9±0.94 in the enriched NH_4^+ treatment. $rETR_{max}$ increased with decreasing pH (ANCOVA; $F_{1, 21} = 12.4760$, $p = 0.0020$). Like $rETR_{max}$, the average F_v/F_m was higher with NH_4^+ enrichment and decreasing pH (ANCOVA; $F_{1, 21} = 29.9680$, $p<0.001$ and ANCOVA; $F_{1, 21} = 10.5410$, $p = 0.0039$, respectively, Fig 4C). The F_v/F_m in the ambient NH_4^+ treatment was 0.59±0.22 and 0.74 ± 0.01 in the enriched NH_4^+ treatment.

The effect of pH on E_k differed between NH_4^+ treatments (ANCOVA; $F_{1, 20} = 4.7757$, $p = 0.00409$, Fig 5A), increasing with decreasing pH in the ambient NH_4^+ treatment, but not the enriched NH_4^+ treatment where there was no relationship between pH and E_k. α was not influenced by pH_T (ANCOVA; $F_{1, 21} = 0.0001$, $p = 0.9938$, Fig 5B). However, α was greater with NH_4^+ enrichment (ANCOVA; $F_{1, 21} = 7.2451$, $p = 0.0137$) with a mean of 0.14±0.03 in the ambient NH_4^+ treatment and a mean of 0.22±0.01 in the enriched NH_4^+ treatment. Likewise, β was not influenced by pH_T (ANCOVA; $F_{1, 21} = 0.0195$, $p = 0.8902$, Fig 5C) but β was

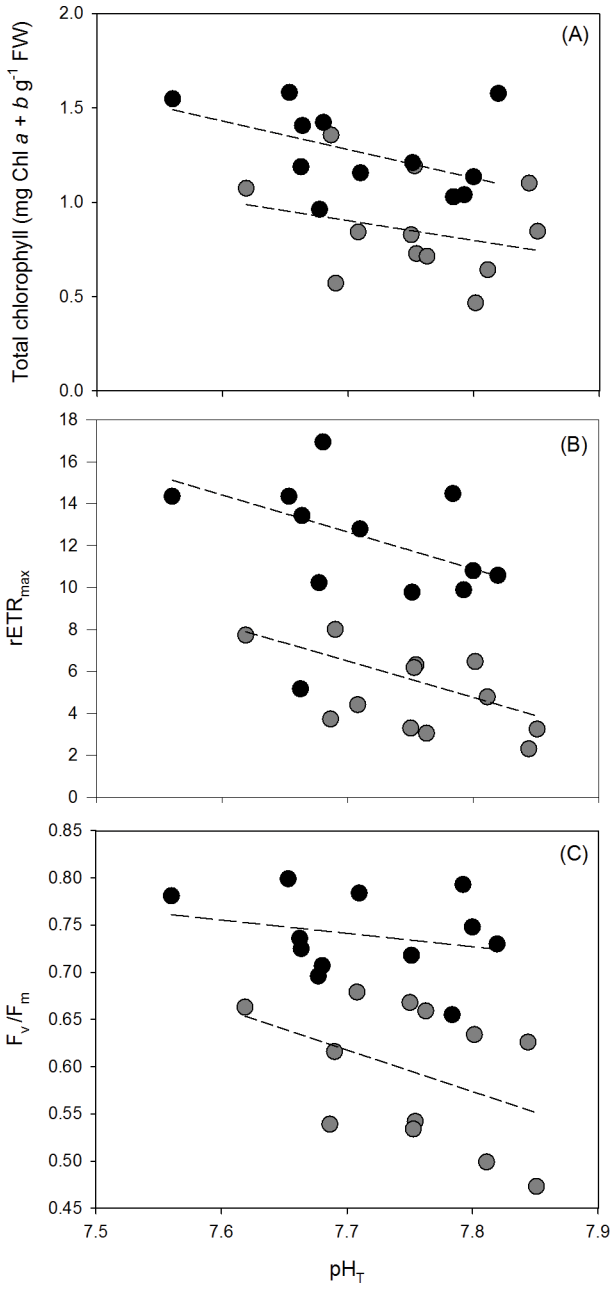

Fig 4. (A) Total chlorophyll (mg Chl *a* + *b* g^{-1} FW), (B) $rETR_{max}$ from rapid light curves, and (C) F_v/F_m from rapid light curves for *Ulva australis* grown under ambient and enriched NH_4^+ treatments across a range of pH_T. Grey points represent ambient NH_4^+ treatments and black points represent enriched NH_4^+ treatments. The slopes of total chlorophyll, $rETR_{max}$, and F_v/F_m with decreasing pH_T for each NH_4^+ treatment (dashed lines) were tested for an interaction using an ANCOVA.

https://doi.org/10.1371/journal.pone.0188389.g004

more negative in the enriched NH_4^+ treatments, averaging -0.008±1.58x10^{-3} in the ambient NH_4^+ treatment and -0.0013±8.48x10^{-4} in the enriched NH_4^+ treatment (ANCOVA; $F_{1, 21}$ = 11.6938, p = 0.0026).

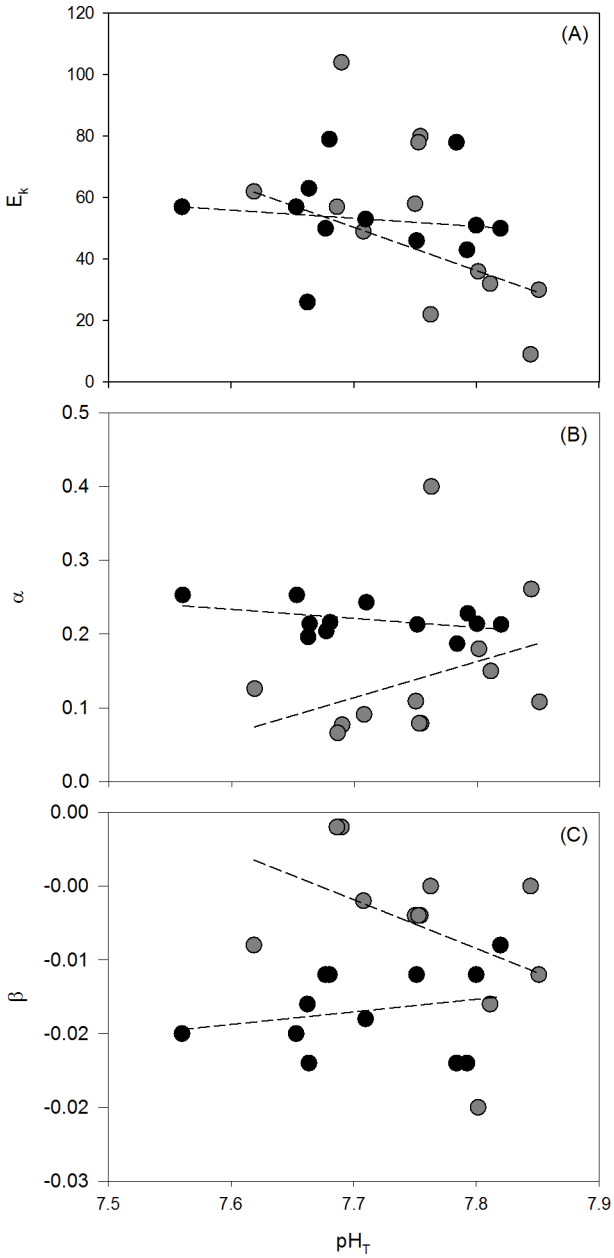

Fig 5. (A) Light saturation point (E_k), (B) initial slope of the curve (α), and (C) slope of photoinhibition at high photon flux densities (β) from rapid light curves for *Ulva australis* grown under ambient and enriched NH_4^+ treatments across a range of pH_T. Grey points represent ambient NH_4^+ treatments and black points represent enriched NH_4^+ treatments. The slopes of E_k, α, and β with decreasing pH_T for each NH_4^+ treatment (dashed lines) were tested for an interaction using an ANCOVA.

https://doi.org/10.1371/journal.pone.0188389.g005

Tissue carbon and nitrogen

Tissue C (% DW) was not affected by pH or NH_4^+ enrichment (ANCOVA; $F_{1, 21} = 0.5377$, $p = 0.4715$ and $F_{1, 21} = 0.6288$ $p = 0.4367$, respectively) (Fig 6A). Tissue N (%DW) averaged 1.39±0.06 in the ambient NH_4^+ treatment and was significantly greater in the enriched NH_4^+ treatment with an average of 2.56±0.14 (ANCOVA; $F_{1, 21} = 62.4082$, $p = <0.001$)(Fig 6B) and increased as pH decreased (ANOVA; $F_{1, 21} = 5.6892$, $p = 0.0266$). The C:N ratio was lower in

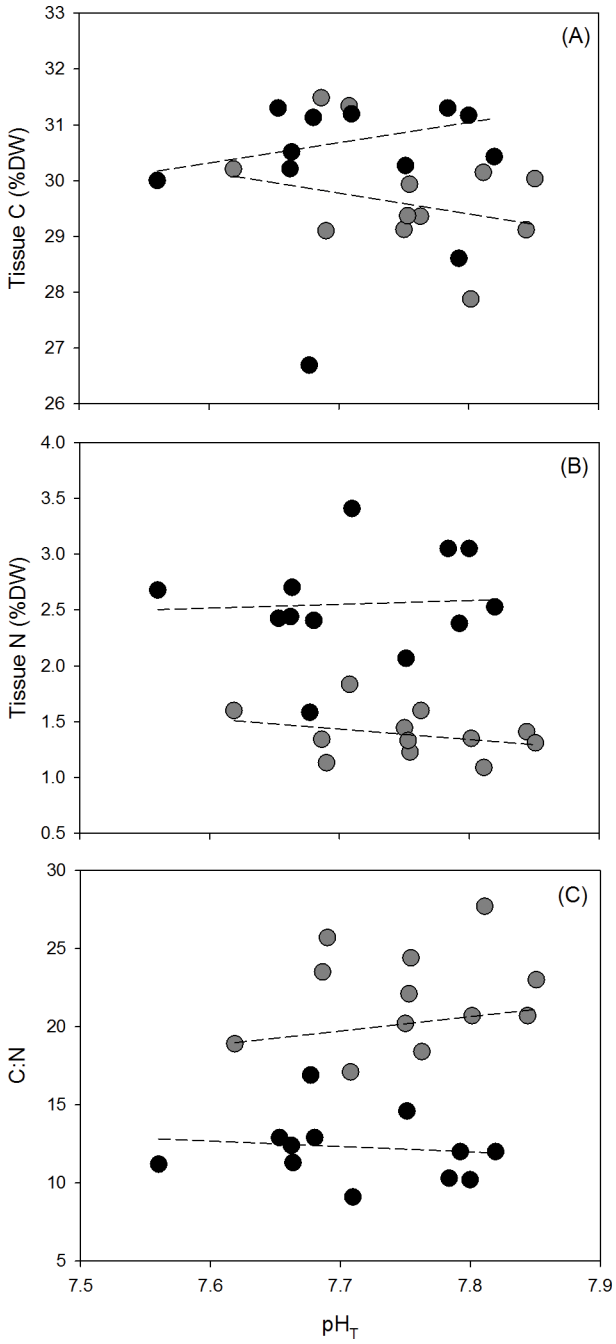

Fig 6. (A) Tissue C (%DW), (B) tissue N (%DW), and (C) C:N ratio of samples of *Ulva australis* under ambient and enriched NH_4^+ treatments across a range of pH_T. Grey points represent ambient NH_4^+ treatments and black points represent enriched NH_4^+ treatments. The slopes of tissue C, tissue N, and the C:N ratio with decreasing pH_T for each NH_4^+ treatment (dashed lines) were tested for an interaction using an ANCOVA.

https://doi.org/10.1371/journal.pone.0188389.g006

enriched NH_4^+ treatment with an average of 11.3±1.15, while in the ambient NH_4^+ treatment the average was 21.87±0.95 (ANCOVA; $F_{1, 21} = 69.5776$, $p = <0.001$)(Fig 6C). The C:N ratio decreased with decreasing pH (ANOVA; $F_{1, 21} = 6.9056$, $p = 0.00157$).

Discussion

The growth, nutrient, and photosynthetic physiology of *Ulva australis* with increased pCO_2/decreased pH did not depend on the NH_4^+ treatment, with the exception of E_k. This was counter to the hypothesis that NH_4^+ enrichment and increased pCO_2/decreased pH would interact to change *U. australis* growth and physiology. This study demonstrates that *U. australis* growth rates are more likely to be influenced by nutrient enrichment, rather than ocean acidification, as NH_4^+ enrichment increased activities of PSII and NH_4^+ pools and ultimately increased growth rates. N-deficiency has been shown to lower the ability of *Ulva rotundata* to photoacclimate to changing light regimes and can lead to declines in $rETR_{max}$ and α in *U. lactuca* [47,48]. NH_4^+ enrichment increased total chlorophyll concentrations, $rETR_{max}$, F_v/F_m, and α increased with NH_4^+ enrichment indicating N-deficiency inhibited photosynthesis. Photoinhibition (β) and differences in β between NH_4^+ enriched and ambient treatments were small at the highest PFDs measured which suggests an increased range of PFD would be better suited for demonstrating effects on β. Nutrient enrichment increased growth and photosynthetic characteristics of *U. australis* which has been shown with many macroalgae [8].

In this study, decreased pH influenced photosynthetic physiology as demonstrated by total chlorophyll, $rETR_{max}$, E_k, and F_v/F_m. With pH being reduced by the addition of pCO_2, the increase in the total dissolved inorganic carbon (DIC) concentration in seawater likely contributed in the increased activity and efficiency of PSII. However, this did not result in increased growth rates. A decoupling of the photosynthetic characteristics and growth rates is not uncommon because growth is linked to multiple components of algal metabolism, not just a single process (i.e., photosynthesis). In this experiment, this decoupling may represent a trade-off between nitrogen resources for improved photosynthetic efficiency (higher concentration of chlorophyll) or growth (resulting in dilution of chlorophyll with cellular division). Here, it was demonstrated that *Ulva australis* grown with NH_4^+ enrichment was better acclimated to various pH conditions with regards to E_k, as there was no relationship between E_k and pH. When grown in the ambient NH_4^+ treatment, E_k increased with increasing CO_2/decreased pH. In future pH conditions, *U. australis* growing in low NH_4^+ seawater may be able to increase their potential habitat range to include those with higher light levels. However, given enough nutrients, light limitations would be reduced and pH would have no effect on E_k.

The supposition that macroalgal growth rates may increase with future pCO_2/pH conditions due to energy savings from downregulation of CCMs [33,49,50] is likely not a pervasive feature of CCM utilizing macroalgae. Enhanced growth with pCO_2 enrichment is probably the result of the influence of light levels on CCMs [51]. Energetic constraints on carbon acquisition at low PFDs increases dependence on passive CO_2 diffusion, while CCMS are more efficient at high PFDs [33]. When PFD is low, the carbon demands of photosynthesis can be saturated by diffusion alone and CCMs are not needed. For example, pCO_2 enrichment only enhanced *Gracilaria lemaneiformis* growth rates at an intermediate PFD [26]. Young and Gobler [32] found that *Ulva* spp. growth rates increased with pCO_2 enrichment but varied by season, primarily increasing only in summer months. Assuming their findings are representative of *Ulva* spp. seasonal growth dynamics in a temperate location, then the results of the current study likely represent a less productive time of year for *U. australis*. Considering other environmental variables such as season, temperature, and light intensity are important for building a comprehensive framework from which we can elucidate patterns of ecological relevance from laboratory studies.

NH_4^+ enrichment increased RGRs to approximately twice that of *Ulva australis* grown in non-enriched seawater. Increased RGR with increasing nutrient concentrations is common for *Ulva* spp. [47,52], but it is also dependent on seasonal changes in light supply and ambient

nitrogen levels [53]. For example, Lapointe and Tenore [54] showed that when *Ulva fasciata* was not grown with sufficient light, the enhancement of growth with NO_3^- was eliminated. Furthermore, growth rates of *Ulva lactuca* more than doubled with the addition of NH_4^+ or NO_3^- when collected from an oligotrophic site, but an increased growth rate with nutrient enrichment was not evident when algae were collected from a nutrient enriched site [55].

In the present experiment, internal NH_4^+ pools and tissue N content were nearly twice as large in the NH_4^+ enriched treatments as in the ambient treatments, indicating light and nutrients were sufficient for nutrient assimilation and growth, while the ambient NH_4^+ treatments were N-limiting. In the NH_4^+ enriched treatment, *Ulva australis* NH_4^+ uptake rates were slower than in the ambient NH_4^+ treatments, which supports the theory that nutrient histories influence nutrient uptake capabilities by feedback inhibition as internal N pools increase [56–61]. *U. australis* from the NH_4^+ enriched treatments, were still capable of NH_4^+ uptake despite growth under high nutrient availability and relatively concentrated NH_4^+ pools. This has also been demonstrated with *Ulva expansa* and *Ulva intestinalis* with varying nutrient histories [61] and shows their ability to take up surplus nutrients under growth with low and high nutrient concentrations.

The increase in tissue N, decrease in the C:N ratio and increase in E_k in the ambient NH_4^+ treatment with decreasing pH in this experiment indicate that decreased pH may provide relief from nutrient limitation. An increase in chlorophyll content and tissue N with decreasing pH support that NH_4^+ was assimilated to produce nitrogenous compounds such as chlorophyll, protein, and amino acids and not stored in internal NH_4^+ pools during this experiment. We did not detect changes in NH_4^+ uptake rates with decreasing pH, which corresponds to the absence of changes in NH_4^+ pools and growth rates. This contrasts that findings of increased NO_3^- uptake rates under future pCO_2/pH conditions in *Ulva rigida*, *Hizikia fusifome*, and *Gracilaria* spp. [15,24,25], and increased NH_4^+ uptake rate future pCO_2/pH in *Hypnea spinella* [62]. The effect of pCO_2/pH on N uptake rate may also be sensitive to temperature, as NO_3^- uptake rates in *Ulva lactuca* increased with CO_2 enrichment at 25˚C, but not 15˚C [21].

Based on our results, it is unlikely NH_4^+ enrichment (a local-scale environmental change) will interact with ocean acidification (a global-scale environmental change), to affect *Ulva australis* growth, nutrient, and photosynthetic physiology. We were able to demonstrate that increased growth rate with NH_4^+ enrichment could be explained by cellular changes in NH_4^+ and photosynthetic physiology. However, physiological responses to pH were more complex, where *Ulva australis* growth rates did not change under future pCO_2/pH conditions, despite the fact that $rETR_{max}$, F_v/F_m, and tissue N increased. These changes in photosynthetic and nutrient physiology could potentially lead to increased growth rates in macroalgae [63]. It was also demonstrated that decreased pH may reduce nutrient limitation and increase E_k under low NH_4^+ conditions. Therefore, growth rates have the potential to increase with future pCO_2/pH conditions under a more favorable set of environmental conditions where PFD and/or season may interact to influence *U. australis* growth rates in future pCO_2/pH conditions. In summary, the concern that ocean acidification may contribute to the increasing the biomass of green-tide blooms along anthropogenically influenced coastlines world-wide is not supported, despite changes in photosynthetic and nutrient physiology that could favor increased growth. However, NH_4^+ enrichment significantly increased growth rates of the opportunistic macroalga *U. australis*. This is likely to contribute to increases in the severity of green-tide blooms in areas where land-use change and development are leading to increases in NH_4^+ concentrations in seawater.

Supporting information

S1 Table. Seawater carbonate chemistry estimates. Measurements of total pH (pH_T) and total alkalinity (AT) are described in the methods. AT was measured as 2111.42 ± 18.33

(mean ± SEM) (n = 7). Salinity is assumed to be 35%. Temperature is assumed to be 16.5˚C (the average temperature throughout the experiment) MFC = mass flow controller.
DIC = dissolved inorganic carbon.
(PDF)

Acknowledgments

We would like to thank Dr. Michael Ellwood (Australia National University) for analyzing the total alkalinity samples and Dr. Gerald Kraft (The University of Melbourne) for helping in the identification of *Ulva australis*. The authors are grateful to the two anonymous reviewers for their thoughtful and constructive feedback that improved the quality of this manuscript.

Author Contributions

Conceptualization: Leah B. Reidenbach, Pamela A. Fernandez, Christina M. McGraw, Catriona L. Hurd, Janet E. Kübler.

Data curation: Leah B. Reidenbach.

Formal analysis: Leah B. Reidenbach.

Funding acquisition: Leah B. Reidenbach, Catriona L. Hurd.

Investigation: Leah B. Reidenbach, Pamela A. Fernandez, Pablo P. Leal, Fanny Noisette.

Methodology: Leah B. Reidenbach, Pamela A. Fernandez, Pablo P. Leal, Fanny Noisette, Christina M. McGraw, Catriona L. Hurd, Janet E. Kübler.

Project administration: Leah B. Reidenbach, Catriona L. Hurd.

Resources: Christina M. McGraw, Andrew T. Revill, Catriona L. Hurd.

Software: Christina M. McGraw, Catriona L. Hurd.

Supervision: Catriona L. Hurd, Janet E. Kübler.

Visualization: Leah B. Reidenbach.

Writing – original draft: Leah B. Reidenbach.

Writing – review & editing: Leah B. Reidenbach, Pamela A. Fernandez, Pablo P. Leal, Fanny Noisette, Christina M. McGraw, Andrew T. Revill, Catriona L. Hurd, Janet E. Kübler.

References

1. IPCC. Climate Change 2013: The Physical Science Basis. 2013. https://doi.org/10.1017/CBO9781107415324
2. Caldeira K, Wickett ME. Ocean model predictions of chemistry changes from carbon dioxide emissions to the atmosphere and ocean. J Geophys Res. 2005; 110: 1–12. https://doi.org/10.1029/2004JC002671
3. Doney SC, Fabry VJ, Feely RA, Kleypas JA. Ocean acidification: the other CO_2 problem. Ann Rev Mar Sci. 2009; 1: 169–192. https://doi.org/10.1146/annurev.marine.010908.163834 PMID: 21141034
4. Raven JA, Caldeira K, Elderfield H, Hoegh-Guldberg O, Liss P, Riebesell U, et al. Ocean acidification due to increasing atmospheric carbon dioxide. 2005; 60.
5. Sabine C, Feely R. In: Reay D, Hewitt N, Grace J, Smith K, editors. Greenhouse Gas Sinks. Oxfordshire: CABI Publishing; 2007. pp. 31–49.
6. Paerl HW. Coastal eutrophication and harmful algal blooms: Importance of atmospheric deposition and groundwater as new nitrogen and other nutrient sources. Limnol Oceanogr. 1997; 42: 1154–1165. https://doi.org/10.4319/lo.1997.42.5_part_2.1154

7. Anderson DM, Glibert P, Burkholder J. Harmful algal blooms and eutrophication: Nutrient sources, compositions, and consequences. Estuaries. 2002; 25: 704–726. https://doi.org/10.1016/j.hal.2008.08.017
8. Valiela I, Mcclelland J, Hauxwell J, Behr PJ, Hersh D, Foreman K. Macroalgal blooms in shallow estuaries: Controls and ecophysiological and ecosystem consequences. Limnol Oceanogr. 1997; 42: 1105–1118. https://doi.org/10.4319/lo.1997.42.5_part_2.1105
9. Teichberg M, Fox SE, Olsen YS, Valiela I, Martinetto P, Iribarne O, et al. Eutrophication and macroalgal blooms in temperate and tropical coastal waters: Nutrient enrichment experiments with *Ulva* spp. Glob Chang Biol. 2010; 16: 2624–2637. https://doi.org/10.1111/j.1365-2486.2009.02108.x
10. Li S, Yu K, Huo Y, Zhang J, Wu H, Cai C, et al. Effects of nitrogen and phosphorus enrichment on growth and photosynthetic assimilation of carbon in a green tide-forming species (*Ulva prolifera*) in the Yellow Sea. Hydrobiologia. Springer International Publishing; 2016; 776: 161–171. https://doi.org/10.1007/s10750-016-2749-z
11. Morand P, Briand X. Excessive Growth of Macroalgae: A Symptom of Environmental Disturbance. Bot Mar. 1996; 39: 491–516. https://doi.org/10.1515/botm.1996.39.1–6.491
12. Ye NH, Zhang XW, Mao YZ, Liang CW, Xu D, Zou J, et al. "Green tides" are overwhelming the coastline of our blue planet: Taking the world's largest example. Ecol Res. 2011; 26: 477–485. https://doi.org/10.1007/s11284-011-0821-8
13. Scherner F, Horta PA, de Oliveira EC, Simonassi JC, Hall-spencer JM, Chow F, et al. Coastal urbanization leads to remarkable seaweed species loss and community shifts along the SW Atlantic. Mar Pollut Bull. Elsevier Ltd; 2013; 76: 106–115. https://doi.org/10.1016/j.marpolbul.2013.09.019 PMID: 24090881
14. Smetacek V, Zingone A. Green and golden seaweed tides on the rise. Nature. 2013; 504: 84–8. https://doi.org/10.1038/nature12860 PMID: 24305152
15. Gordillo FJL, Niell FX, Figueroa FL. Non-photosynthetic enhancement of growth by high CO2 leve in the nitrophilic seawed *Ulva rigida* C. Agardh (Chlorophyta). Plantad. 2001; 213: 64–70. https://doi.org/10.1007/s004250000468
16. Gordillo FJL, Figueroa FL, Niell FX. Photon- and carbon-use efficiency in *Ulva rigida* at different CO_2 and N levels. Planta. 2003; 218: 315–322. https://doi.org/10.1007/s00425-003-1087-3 PMID: 12937985
17. Russell BD, Thompson JAI, Falkenberg LJ, Connell SD. Synergistic effects of climate change and local stressors: CO_2 and nutrient-driven change in subtidal rocky habitats. Glob Chang Biol. 2009; 15: 2153–2162. https://doi.org/10.1111/j.1365-2486.2009.01886.x
18. Hofmann LC, Straub S, Bischof K. Elevated CO_2 levels affect the activity of nitrate reductase and carbonic anhydrase in the calcifying rhodophyte *Corallina officinalis*. J Exp Bot. 2013; 64: 899–908. https://doi.org/10.1093/jxb/ers369 PMID: 23314813
19. Hofmann LC, Heiden J, Bischof K, Teichberg M. Nutrient availability affects the response of the calcifying chlorophyte *Halimeda opuntia* (L.) J.V. Lamouroux to low pH. Planta. 2014; 239: 231–242. https://doi.org/10.1007/s00425-013-1982-1 PMID: 24158465
20. Liu C, Dinghui Z. Effects of elevated CO_2 on the photosynthesis and nitrate reductase activity of *Pyopia haitanensis* (Bangiales, Rhodophyta) grown at different nutrient levels. Chinese J Oceanol Limnol. 2015; 33: 419–429. https://doi.org/10.1007/s00343-015-4057-2
21. Liu C, Zou D. Responses of elevated CO_2 on photosynthesis and nitrogen metabolism in *Ulva lactuca* (Chlorophyta) at different temperature levels. Mar Biol Res. 2015; 1000: 1–10. https://doi.org/10.1080/17451000.2015.1062520
22. Kang JW, Chung IK. The effects of eutrophication and acidification on the ecophysiology of *Ulva pertusa* Kjellman. J Appl Phycol. Journal of Applied Phycology; 2017; 1–9. https://doi.org/10.1007/s10811-017-1087-5
23. Turpin DH. Effects of Inorganic N availability on algal photosynthesis and carbon metabolism. Journal of Phycology. 1991. pp. 14–20. https://doi.org/10.1111/j.0022-3646.1991.00014.x
24. Zou D. Effects of elevated atmospheric CO_2 on growth, photosynthesis and nitrogen metabolism in the economic brown seaweed, *Hizikia fusiforme* (Sargassaceae, Phaeophyta). Aquaculture. 2005; 250: 726–735. https://doi.org/10.1016/j.aquaculture.2005.05.014
25. Gao K, Aruga Y, Asada K, Kiyohara M. Influence of enhanced CO_2 on growth and photosynthesis of the red algae *Gracilaria* sp. and *G. chilensis*. J Appl Phycol. 1993; 5: 563–571. https://doi.org/10.1007/BF02184635
26. Zou D, Gao K. Effects of elevated CO_2 on the red seaweed *Gracilaria lemaneiformis* (Gigartinales, Rhodophyta) grown at different irradiance levels. Phycologia. 2009; 48: 510–517. https://doi.org/10.2216/08-99.1.The

27. Israel A, Hophy M. Growth, photosynthetic properties and Rubisco activities and amounts of marine macroalgae grown under current and elevated seawater CO_2 concentrations. Glob Chang Biol. 2002; 8: 831–840. https://doi.org/10.1046/j.1365-2486.2002.00518.x

28. Olischläger M, Bartsch I, Gutow L, Wiencke C. Effects of ocean acidification on growth and physiology of *Ulva lactuca* (Chlorophyta) in a rockpool-scenario. Phycol Res. 2013; 61: 180–190. https://doi.org/10.1111/pre.12006

29. Andría JR, Brun FG, Pérez-Lloréns JL, Vergara JJ. Acclimation responses of Gracilaria sp. (Rhodophyta) and Enteromorpha intestinalis (Chlorophyta) to changes in the external inorganic carbon concentration. Bot Mar. 2001; 44: 361–370. https://doi.org/10.1515/BOT.2001.046

30. Rautenberger R, Fernández PA., Strittmatter M, Heesch S, Cornwall CE, Hurd CL, et al. Saturating light and not increased carbon dioxide under ocean acidification drives photosynthesis and growth in *Ulva rigida* (Chlorophyta). Ecol Evol. 2015; 5: 874–888. https://doi.org/10.1002/ece3.1382 PMID: 25750714

31. Giordano M, Beardall J, Raven JA. CO_2 concentrating mechanisms in algae: mechanisms, environmental modulation, and evolution. Annu Rev Plant Biol. 2005; 56: 99–131. https://doi.org/10.1146/annurev.arplant.56.032604.144052 PMID: 15862091

32. Young CS, Gobler CJ. Ocean acidification accelerates the growth of two bloom-forming macroalgae. PLoS ONE. 2016; 11: 1–21. https://doi.org/10.1371/journal.pone.0155152 PMID: 27176637

33. Hepburn CD, Pritchard DW, Cornwall CE, Mcleod RJ, Beardall J, Raven JA, et al. Diversity of carbon use strategies in a kelp forest community: Implications for a high CO_2 ocean. Glob Chang Biol. 2011; 17: 2488–2497. https://doi.org/10.1111/j.1365-2486.2011.02411.x

34. Cornwall CE, Revill AT, Hall-spencer JM, Milazzo M, Raven JA, Hurd CL. Inorganic carbon physiology underpins macroalgal responses to elevated CO_2. Nat Publ Gr. Nature Publishing Group; 2017; 1–12. https://doi.org/10.1038/srep46297

35. Chen B, Zou D, Ma J. Interactive effects of elevated CO_2 and nitrogen-phosphorus supply on the physiological properties of *Pyropia haitanensis* (Bangiales, Rhodophyta). J Appl Phycol. 2016; 28: 1235–1243. https://doi.org/10.1007/s10811-015-0628-z

36. Syrett PJ. Nitrogen Metabolism of Microalgae. Can J Fish Aquat Sci. 1981; 210: 182–210.

37. Paerl HW, Piehler MF. Nitrogen and marine eutrophication. In: Capone DG, Bronk DA, Mulholland MR, Carpenter EJ, editors. Nitrogen in the marine environment, 2. Elsevier. 2008. pp 529–567

38. McGraw CM, Cornwall CE, Reid MR, Currie KI, Hepburn CD, Boyd PW, et al. An automated pH-controlled culture system for laboratory-based ocean acidification experiments. Limnol Oceanogr Methods. 2010; 8: 686–694. https://doi.org/10.4319/lom.2010.8.686

39. Bockmon EE, Frieder CA, Navarro MO, White-Kershek LA, Dickson AG. Technical Note: Controlled experimental aquarium system for multi-stressor investigation of carbonate chemistry, oxygen saturation, and temperature. Biogeosciences. 2013; 10: 5967–5975. https://doi.org/10.5194/bg-10-5967-2013

40. Dickson AG, Sabine CL, Christian JR. Guide to Best Practices for Ocean CO2 Measurements. 2007.

41. Hurd CL. Water motion, marine macroalgal physiology, and production. J Phycol. 2000; 36: 453–472. https://doi.org/10.1046/j.1529-8817.2000.99139.x

42. Pedersen MF. Transient ammonium uptake in the macroalgae *Ulva lactuca* (Chlorophyta): Nature, regulation, and the consequences for choice of measuring technique. J Phycol. 1994; 30: 980–986.

43. Hurd CL, Harrison PJ, Druehl LD. Effect of seawater velocity on inorganic nitrogen uptake by morphologically distinct forms of *Macrocystis integrifolia* from wave-sheltered and exposed sites. Mar Biol. 1996; 126: 205–214. https://doi.org/10.1007/BF00347445

44. Ritchie RJ. Universal chlorophyll equations for estimating chlorophylls a, b, c, and d and total chlorophylls in natural assemblages of photosynthetic organisms using acetone, methanol, or ethanol solvents. Photosynthetica. 2008; 46: 115–126. https://doi.org/10.1007/s11099-008-0019-7

45. Baker NR. Chlorophyll fluorescence: A probe of photosynthesis *in vivo*. Annu Rev Plant Biol. 2008; 59: 89–113. https://doi.org/10.1146/annurev.arplant.59.032607.092759 PMID: 18444897

46. Walsby AE. Numerical integration of phytoplankton photosynthesis through time and depth in a water column. New Phytol. 1997; 136: 189–209. https://doi.org/10.1046/j.1469-8137.1997.00736.x

47. Dailer ML, Smith JE, Smith CM. Responses of bloom forming and non-bloom forming macroalgae to nutrient enrichment in Hawai'i, USA. Harmful Algae. Elsevier B.V.; 2012; 17: 111–125. https://doi.org/10.1016/j.hal.2012.03.008

48. Chen B, Zou D, Jiang H. Elevated CO_2 exacerbates competition for growth and photosynthesis between *Gracilaria lemaneiformis* and *Ulva lactuca*. Aquaculture. Elsevier B.V.; 2015; 443: 49–55. https://doi.org/10.1016/j.aquaculture.2015.03.009

49. Raven JA, Giordano M, Beardall J, Maberly SC. Algal and aquatic plant carbon concentrating mechanisms in relation to environmental change. Photosynth Res. 2011; 109: 281–296. https://doi.org/10.1007/s11120-011-9632-6 PMID: 21327536

50. Koch M, Bowes G, Ross C, Zhang XH. Climate change and ocean acidification effects on seagrasses and marine macroalgae. Glob Chang Biol. 2013; 19: 103–132. https://doi.org/10.1111/j.1365-2486.2012.02791.x PMID: 23504724

51. Kübler JE, Raven JA. The interaction between inorganic carbon acquisition and light supply in *Palmaria palmata* (Rhodophyta). J Phycol. 1995; 31: 369–375.

52. Fong P, Fong JJ, Fong CR. Growth, nutrient storage, and release of dissolved organic nitrogen by *Enteromorpha intestinalis* in response to pulses of nitrogen and phosphorus. Aquat Bot. 2004; 78: 83–95. https://doi.org/10.1016/j.aquabot.2003.09.006

53. Fong P, Boyer KE, Zedler JB. Developing an indicator of nutrient enrichment in coastal estuaries and lagoons using tissue nitrogen content of the opportunistic alga, *Enteromorpha intestinalis* (L. Link). J Exp Mar Bio Ecol. 1998; 231: 63–79. https://doi.org/10.1016/S0022-0981(98)00085-9

54. Lapointe BE, Tenore KR. Experimental outdoor studies with *Ulva fasciata* Delile. I. Interaction of light and nitrogen on nutrient uptake, growth, and biochemical composition. J Exp Mar Bio Ecol. 1981; 53: 135–152. https://doi.org/10.1016/0022-0981(81)90015-0

55. Teichberg M, Fox SE, Aguila C, Olsen YS, Valiela I. Macroalgal responses to experimental nutrient enrichment in shallow coastal waters: Growth, internal nutrient pools, and isotopic signatures. Mar Ecol Prog Ser. 2008; 368: 117–126. https://doi.org/10.3354/meps07564

56. D'Elia CF, DeBoer JA. Nutritional studies of two red algae. II. Kinetics of ammonium and nitrate uptake. J Phycol. 1978; 14: 266–272. https://doi.org/10.1111/j.1529-8817.1978.tb00297.x

57. Fujita RM. The role of nitrogen status in regulating ammonium transient uptake and nitrogen storage by macroalgae. J Exp Mar Bio Ecol. 1985; 92: 283–301. https://doi.org/10.1016/0022-0981(85)90100-5

58. McGlathery KJ, Pedersen MF, Borum J. Changes in intracellular nitrogen pools and feedback controls on nitrogen uptake in *Chaetomorpha linum* (Chlorophyta)1. J Phycol. 1996; 32: 393–401. https://doi.org/10.1111/j.0022-3646.1996.00393.x

59. Fong P, Boyer KE, Kamer K, Boyle KA. Influence of initial tissue nutrient status of tropical marine algae on response to nitrogen and phosphorus additions. Mar Ecol Prog Ser. 2003; 262: 111–123. https://doi.org/10.3354/meps262111

60. Teichberg M, Heffner LR, Fox S, Valiela I. Nitrate reductase and glutamine synthetase activity, internal N pools, and growth of *Ulva lactuca*: Responses to long and short-term N supply. Mar Biol. 2007; 151: 1249–1259. https://doi.org/10.1007/s00227-006-0561-4

61. Kennison RL, Kamer K, Fong P. Rapid nitrate uptake rates and large short-term storage capacities may explain why opportunistic green macroalgae dominate shallow eutrophic estuaries. J Phycol. 2011; 47: 483–494. https://doi.org/10.1111/j.1529-8817.2011.00994.x PMID: 27021977

62. Suarez-Alvarez S, Gomez-Pinchetti JL, Garcia-Reina G. Effects of increased CO_2 levels on growth, photosynthesis, ammonium uptake and cell composition in the macroalga *Hypnea spinella* (Gigartinales, Rhodophyta). J Appl Phycol. 2012; 24: 815–823. https://doi.org/10.1007/s10811-011-9700-5

63. Kroeker KJ, Kordas RL, Crim RN, Hendriks IE, Ramajo L, Singh GS, et al. Impacts of ocean acidification on marine organisms: Quantifying sensitivities and interaction with warming. Glob Chang Biol. 2013; 19: 1884–1896. https://doi.org/10.1111/gcb.12179 PMID: 23505245